HHS Public Access

Author manuscript

*Brain Struct Funct*. Author manuscript; available in PMC 2019 July 13.

Published in final edited form as:

*Brain Struct Funct*. 2018 September ; 223(7): 3169–3181. doi:10.1007/s00429-018-1673-6.

# Adolescent isolation rearing produces a prepulse inhibition deficit correlated with expression of the NMDA GluN1 subunit in the nucleus accumbens

**Megan L. Fitzgerald**[1,2] and **Virginia M. Pickel**[1]

[1]Brain and Mind Research Institute, Weill Cornell Medicine, 407 East 61st Street, New York, NY 10065, USA

[2]New York State Psychiatric Institute, Columbia University, New York, NY 10032, USA

## Abstract

Adolescence is a transition period during which social interaction is necessary for normal brain and behavior development. Severely abnormal social interactions during adolescence can increase the incidence of lifelong psychiatric disease. Decreased prepulse inhibition (PPI) is a quantifiable hallmark of some psychiatric illnesses in humans and can be elicited in rodents by isolation rearing throughout the adolescent transition period. PPI is a measure of sensorimotor gating in which the nucleus accumbens (Acb) is crucially involved. The Acb is comprised of core and shell subregions, which receive convergent dopaminergic and glutamatergic inputs. To gain insight into the neurobiological correlates of adolescent adversity, we conducted electron microscopic immunolabeling of dopamine D1 receptors (D1Rs) and the GluN1 subunit of glutamate NMDA receptors in the Acb of isolation-reared (IR) adult male rats. In all animals, GluN1 was primarily located in dendritic profiles, many of which also contained D1Rs. GluN1 was also observed in perisynaptic glia and axon terminals. In IR rats compared with group-reared controls, GluN1 density was selectively decreased in D1R-containing dendrites of the Acb core. Across all animals, dendritic GluN1 density correlated with average percent PPI, implicating endogenous expression of NMDA receptors of the Acb as a possible substrate of the PPI response. These results suggest that adolescent isolation dampens NMDA-mediated excitation in direct (D1R-containing) output neurons of the Acb, and that these changes influence the operational measure of PPI.

### Keywords

NMDA receptor; D1 receptor; Sensorimotor gating; Social isolation; Adolescence; Electron microscopy

vpickel@med.cornell.edu, missfitz@gmail.com.

**Conflict of interest** The authors declare that they have no conflicts of interest.

**Human/animal rights** This article does not contain any studies with human participants performed by any of the authors. All procedures involving animals were carried out in accordance with the National Institutes of Health Guidelines for the Care and Use of Laboratory Animals, and were approved by the Institutional Animal Care and Use Committees (IACUC) at Weill-Cornell Medical College. Every effort was made to minimize the number of animals used and their suffering.

## Introduction

Adolescence is a period of development during which social mammals are uniquely sensitive to peer interactions. Social isolation during adolescence, whether in humans or rodent models, results in negative behavioral traits that last throughout life and cut across the symptoms of multiple psychiatric disorders (Sebastian et al. 2010; Somerville et al. 2010). These traits include impaired prepulse inhibition (PPI) (Swerdlow et al. 2000; Schubert et al. 2009). PPI is a quantifiable measure of sensorimotor gating found to be defective in schizophrenia and several other psychiatric disorders (Braff et al. 2001; Swerdlow et al. 2006).

Isolation rearing of male rats throughout adolescence generates an enduring PPI deficit in adulthood, which is dependent upon the period of isolation encapsulating adolescent development (Wilkinson et al. 1994; Bakshi and Geyer 1999). Sensorimotor gating is not disrupted if rats are socially isolated as adults (Wilkinson et al. 1994), indicating that the neural circuitry mediating PPI is highly responsive to the loss of rewarding peer–peer interactions specifically during adolescent development.

The nucleus accumbens (Acb) is a subcortical brain region that is finely tuned to the rewarding effects of social interactions during adolescence (Somerville et al. 2010) and also critically regulates PPI (Swerdlow et al. 2000). The Acb is composed of motor-associated core and reward-associated shell subregions which are highly interconnected (Zahm 2000). Neural activity in both core and shell is regulated by synaptic inputs from cortical and subcortical glutamatergic and midbrain dopaminergic inputs (Brog et al. 1993; Groenewegen et al. 1999). The ventromedial Acb core and shell are potently targeted by glutamatergic inputs from the prelimbic prefrontal cortex (Berendse et al. 1992), a brain region that continues to develop over adolescence and is impacted by isolation rearing (Day-Wilson et al. 2006; Fitzgerald et al. 2013).

Altered glutamate and dopamine indices in the Acb have been observed in isolation-reared rodents (Fone and Porkess 2008; Wood et al. 2005). Conversely, direct manipulation of Acb dopamine and glutamate neurotransmission induces PPI deficits: a PPI deficit in rats can be pharmacologically elicited by (1) direct blockade of glutamate NMDA receptors in the Acb (Reijmers et al. 1995), (2) injection of dopa-mine into the rat Acb core (Swerdlow et al. 1990), or (3) intra-accumbens infusion of apomorphine, a D1/D2 receptor antagonist (Broersen et al. 1999). Dopamine depletion in the Acb rescues the isolation-induced PPI deficit (Powell et al. 2003). The dopamine D1 receptor is co-localized with the obligatory NMDA receptor subunit GluN1 in postsynaptic compartments of the Acb shell and core (Hara and Pickel 2005, 2009). Additionally, the D1 receptor forms a heterodimer with the GluN1 subunit of the NMDA receptor, resulting in a receptor complex that may mediate desensitization of the D1 receptor (Fiorentini et al. 2003). This evidence suggests that convergent glutamatergic and dopaminergic signaling pathways in the Acb regulate the operational measure of PPI, and that these might be altered by adolescent social isolation.

We used behavioral measures and electron microscopic immunolabeling to test the hypothesis that PPI deficits in IR rats correlate with glutamate NMDA receptor availability

in dopamine-responsive neurons of the Acb core and shell. To do so, we used adult male Sprague–Dawley rats that were reared alone in single cages (isolation) or in groups of three from weaning to adulthood and behaviorally tested for a PPI deficit prior to electron microscopic analysis. Immunogold-silver was used to identify and quantitatively analyze GluN1 subunits of the NMDA receptor. Neuronal compartments containing D1R were labeled with immunoperoxidase. GluN1 immunogold counts were conducted in postsynaptic dendrites with and without D1 receptor labeling in the Acb core and shell of group and IR adult rats. We could thereby test the hypothesis that IR induces changes in Acb glutamatergic and dopaminergic transmitter systems, which may ultimately disrupt the balance necessary for effective sensorimotor gating (Ramocki and Zoghbi 2008).

## Materials and methods

### Animals and housing

Male Sprague–Dawley rats were obtained commercially from Taconic Farms (Hudson, NY) after weaning at post-natal day (PD) 21. After 1 day of acclimatization to our animal facility, rat pups were randomly assigned for housing either in isolation (one animal/cage; $n = 9$) or in small groups (three animals/cage; $n = 9$) for 8 weeks, spanning the pre-pubertal period through early adulthood (Spear 2000). All animals were kept in a temperature- and humidity-controlled environment and maintained with HEPA-filtered air on a 12-h light/dark cycle (lights on from 7am to 7pm). Food and water were available ad libitum.

### PPI testing

At the end of the 8-week period, at PD77, the young adult rats were tested for auditory-evoked PPI, determined by the reduction in response to a startle-eliciting stimulus (pulse) when preceded by a weaker stimulus (prepulse). PPI test sessions were performed as described in detail previously (Fitzgerald et al. 2013). Briefly, an SR-LAB startle apparatus (San Diego Instruments, San Diego, CA) was used to test PPI in all rats. Background noise and acoustic stimuli were generated using a Radioshack Supertweeter mounted inside the isolation cabinet. The rats were placed in the startle chamber and acclimated to 65 dB background noise for 5 min. The first six acoustic stimuli were startle-eliciting pulses of 40 ms bursts of 120 dB noise. Prepulses were 20 ms stimuli 3, 6, or 12 dB above the 65 dB background noise prior to the acoustic pulse and were presented five times each in a pseudorandom sequence with ten pulse-alone stimuli. Inter-stimuli intervals ranged between 8 and 23 s, averaging 15 s. Five more pulse-alone stimuli concluded the session. Percent PPI was calculated as: %PPI = (average startle magnitude to XdB prepulse + pulse stimulus)/(average startle magnitude to pulse-alone trials) × 100. The first six pulse-alone stimuli were treated as part of the acclimatization process and not included in averages because of highly variable and potentiated initial startle responses. A single animal (Rat 1, group-reared) was unfortunately unable to be used in the PPI analysis because unforeseen loud drilling and construction noise disrupted the behavioral testing. This animal, however, was included in all electron microscopy analyses.

Percent PPI was calculated for each animal at each pre-pulse volume (3, 6, and 12 dB). Average PPI was calculated for each animal using all-combined prepulse trials. An unpaired

*t* test was used to compare the PPI response of group and isolation-reared animals. Significance was determined using a two-tailed *P* value of < 0.05. An *F* test was used to compare variances.

## Fixation and tissue preparation

After completion of PPI testing, all rats were returned to their home cages prior to sacrifice. Rats were deeply anesthetized by intraperitoneal injection of sodium pentobarbital (150 mg/kg). The brain tissue of the anesthetized rats was fixed by aortic arch perfusion using a Masterflex pump (Barnat Company, Barrington, IL, USA) to sequentially deliver (1) 1–5 ml of normal saline (0.9%) containing 1000 units/ml of heparin, (2) 40 ml of 0.1 M phosphate buffer (PB; pH 7.4) containing 3.75% acrolein and 2% paraformaldehyde, and (3) 150 ml of 2% paraformaldehyde in PB. After removing the brain from the cranium, the forebrain was sliced into approximately 5 mm coronal slabs of tissue that was post fixed for 30 min in 2% paraformaldehyde in PB. A Leica Vibratome (Leica Microsystems, Bannockburn, IL, USA) was used to cut 40-μm-thick coronal sections through the ventral striatum. These were collected at 1.6 mm anterior to Bregma, as referenced in the rat brain atlas (Paxinos and Watson 1998).

## Antisera

The dopamine D1 receptor was labeled using a commercially available rat monoclonal antibody from Sigma (St. Louis, MO). The antibody was raised against a 97 amino acid peptide sequence corresponding to the C terminus of the human D1 receptor. This antibody has been well-characterized: its selectivity for the antigenic protein has been demonstrated through Western blot, immunoprecipitation, and blocking control experiments (Levey et al. 1993). The D1 receptor antibody was used at a 1:100 dilution for immunoperoxidase labeling.

The GluN1 subunit of the NMDA receptor was identified through a commercially available affinity-purified polyclonal rabbit antiserum raised against a 30 amino acid peptide sequence corresponding to the C terminus of rat GluN1 from Chemicon International (lot number 22050268, received 5/10/02, Temecula, CA). Specificity and selectivity of this antibody and lot have been confirmed in a conditional GluN1 knockout mouse model (Glass et al. 2008). The GluN1 antibody was used at a 1:75 dilution for immunogold labeling.

## Electron microscopic immunolabeling

Tissue sections containing the ventral striatum from group-and isolation-reared adult rats were co-processed for dual immunogold and immunoperoxidase labeling of GluN1 and D1R, respectively. The immunolabeling method was a modification of that described by Milner (2011). The tissue was incubated overnight (4 °C) plus 24 h (room temperature) in a 0.1 M Tris-buffered saline (TS) solution containing the D1R and GluN1 antisera. Subsequently, the tissue was washed through several changes of TS and incubated for 30 min in a TS solution containing 0.1% bovine serum albumin (BSA) and horse anti-rat biotinylated IgG (1:400; Jackson) for identification of the rat D1R. The biotinylated IgG was then detected by incubation of the tissue using the Vector Stain ABC Elite kit (Vector Laboratories, Burlingame, CA). The peroxidase reaction product was visualized by reaction

for 6 min in 3,3′-diaminobenzadine (DAB, Sigma-Aldrich, St. Louis, MO) with 0.1% hydrogen peroxide. Following the DAB reaction, these sections were washed in TS, and incubated for 2 h in a 1:50 dilution of ultrasmall gold (Electron Microscopy Sciences, Hatfield, PA) conjugated to donkey anti-rabbit IgG. The sections were rinsed in 0.1 M PBS, post fixed with 2% glutaraldehyde in 0.1 M PB for 10 min, rinsed in 0.1 M PB, and then rinsed in 0.2 M citric acid. The gold particles were visualized using the Silver IntensEM kit (GE Healthcare, Piscataway, NJ), reacting for 7 min at room temperature. Silver-intensified sections were rinsed in 0.2 M citrate buffer followed by a second rinse in 0.1 M PB, and a 1 h incubation in 2% osmium tetroxide in 0.1M PB before embedding in epoxy resin between sheets of Aclar plastic using conventional electron microscopic methods (Leranth and Frotscher 1989) and the Embed 812 kit (Electron Microscopy Sciences. Hatfield, PA).

## Micrograph acquisition

Ultrathin sections through the ventromedial Acb shell and core (directly medial to the anterior commissure) were cut from flat-embedded Vibratome sections using a Leica ultramicrotome, as described and diagrammed by Hara and Pickel (2009). These ultrathin sections were counterstained with uranyl acetate and lead citrate prior to examination with an FEI CM-10 transmission electron microscope. Electron microscopic images were captured by an investigator blind to whether the tissue was derived from group- or isolation-reared animals.

Immunoperoxidase labeling was regarded as positive when the electron dense precipitate in individual profiles was greater than that seen in other morphologically similar profiles in the neuropil. Immunogold-labeled structures were identified as those containing one or more gold particles. Although thus including all labeled profiles in the analysis might risk inclusion of a few profiles that contain non-specific labeling, we opted to analyze in this manner to avoid experimental bias against smaller structures such as dendritic spines which, because of their size, contain fewer immunogold deposits than larger-sized profiles with similar receptor density. This method was validated in part by the observation that our immunogold-labeled tissue lacked spurious gold–silver deposits overlying myelin and other structures not known to contain GluN1.

Quantitative comparisons of the distribution of GluN1 immunolabeling in the Acb of isolated and group-reared rats were conducted independently in tissue defined as belonging to a specific subgroup only after completion of the data acquisition. For this, we examined thin sections that were collected equally from the surface of one vibratome section through the Acb subregions. Micrographs were captured where immunolabeling for both antisera was visible in the same field to avoid the possible confound of varying immunogold/immunoperoxidase penetration depths. These neuronal profiles included dendrites and dendritic spines, glia, small (< 0.15 μm cross-sectional diameter) axons typically containing neurotubules, but few if any vesicular organelles, and large (> 0.15 μm cross-sectional) vesicle-filled axon terminals that were without recognizable synapses or formed either asymmetric or symmetric synapses with defined targets. Micrographs were examined to determine the (1) number of D1 and/or GluN1-labeled profiles in a given neuropil area, and (2) subcellular location of individual immunogold-silver deposits identifying GluN1 in

dendritic or axonal compartments. Microscopic illustrations were prepared by importing digital images into Adobe Photoshop (CS4) and Powerpoint (Microsoft Office, 2007) to enhance contrast, prepare composite plates, and add lettering.

## Data analysis

Micrographs were analyzed by an investigator blind to rearing condition. A total of 1508 micrographs (representing 54,195 $\mu m^2$ neuropil) were analyzed from the Acb core of group-reared- and isolated rats, and 1514 micrographs (54,170 $\mu m^2$ neuropil) were analyzed from the Acb shell. MCID Elite software Version 6.0 (Imaging Research Inc., Ontario, Canada) was used to measure the diameter, major axis and minor axis length, perimeter, area, and form factor of immunolabeled neuronal profiles. Measures were conducted by tracing each profile by hand. Because dendritic shafts are roughly cylindrical in nature, and have a fairly regular form (unlike axon terminals and glial profiles), dendritic immunogold density can be calculated in dendritic profiles and compared between groups. GluN1 immunogold density in axon terminals and glial profiles was unable to be accurately determined because of the irregular shapes of these profiles, and, therefore, GluN1 density between isolates and controls in these cell types were not able to be compared in the current study. To avoid bias against any neuronal population that might be more typically represented by longitudinal cuts through the Acb, dendrites were not eliminated based upon form factor (i.e., length to width ratio). However, dendrites that extended beyond a single micrograph field were not counted. While immunogold density is not a fully quantitative measure representative of the absolute number of GluN1 subunits within the neuropil, calculating GluN1 immunogold density in this manner allows an examination of relative GluN1 expression between groups and individual subjects within a study at a subcellular resolution not accessible through other techniques.

## Statistical analysis

To test the hypothesis that isolation rearing alters postsynaptic GluN1 expression, MCID and Excel computer software (Version 12.3.2 for Mac) were first used to calculate animal averages of GluN1 immunogold density in D1-containing and non-D1-containing dendrites and dendritic spines. An unpaired *t* test was used to determine differences in GluN1 density in dendritic profiles between isolated and group-reared rats. Statistical significance was determined at $p < 0.05$. An *F* test was used to test variance between groups, and Welsh's correction was used in the case that variances between groups were found to be significantly different.

To test the hypothesis that PPI correlates with the degree of expression of NMDA receptors in dendritic profiles of the Acb, linear regression analysis was used. We chose to use average %PPI rather than 6 dB %PPI values in our regression analyses in order (1) increase the number of PPI trials used in the calculation of %PPI per animal, (2) avoid experimental bias that could result from choosing a single decibel point to test the overall correlation of sensorimotor gating with Acb GluN1 dendritic density. Separate analyses were undertaken for shell and core, and for dendrites that did and did not contain D1R. GluN1 immunogold density was correlated with average %PPI values from the same animal using the linear

regression analysis function of Prism 5 for Mac OS X (Version 5.0a). Significance was determined at $p < 0.05$.

## Results

### Acb dendrites containing GluN1 and/or D1 receptors are targets of inhibitory and excitatory synaptic inputs

In both isolated and group-reared animals, GluN1 immunogold particles were primarily contained in somata, dendrites, and dendritic spines of the Acb core and shell (Fig. 1a, b). This distribution was similar to that previously reported by our laboratory (Hara and Pickel 2005), and was similar when the immunoperoxidase and immunogold labels were reversed (data not shown). While dual-labeled dendrites were frequently observed, singly labeled D1 and GluN1 dendrites were also common in the Acb shell and core (Fig. 2a–h). GluN1 immunogold labeling was associated with both non-synaptic and synaptic portions of the dendritic plasma membrane. All of the labeled dendritic shafts, but none of the labeled dendritic spines, contained mitochondria, endomembranes, multivesicular bodies, and other cytoplasmic organelles.

When synaptic input to GluN1-containing dendrites formed symmetric inhibitory-type junctions, or did not have a visible postsynaptic specialization, immunogold particles were more commonly located distal to the point of synaptic input, towards the interior of the dendrite (Figs. 2a, c, g, 3a–d). This labeling may indicate NMDA receptors responsive to excitatory-type synaptic input emanating from a different site, or trafficking of the receptors. Presynaptic terminals providing input to labeled dendrites contained small clear synaptic vesicles, or a combination of small clear vesicles and one or more large dense-core vesicles.

In both the core and shell, GluN1- and/or D1-containing dendritic spines frequently had a visible spine apparatus, indicating excitatory-type input (Fig. 3e–h). The majority of excitatory-type synaptic input targeted dendritic spines; however, asymmetric postsynaptic densities indicative of glutamatergic terminals were also visible on dendritic shaft profiles, some of which contained D1 and/or GluN1 (Fig. 2b, d, f, h).

### Axonal profiles contain GluN1

Although the majority of GluN1 labeling was contained within somata, dendrites, and dendritic spines, some GluN1 labeling was also seen in axonal and perisynaptic glial profiles in the Acb shell and core of all rats. GluN1 immuno-gold was contained within both symmetric inhibitory-type and asymmetric excitatory-type axon terminals. These axon terminals formed synapses with dendrites, some of which also contained GluN1 immunogold and/or D1 immunoperoxidase (Fig. 4a–d). In terminals that did not form a visible synapse within the plane of section, and in terminals that formed inhibitory-type synapses, GluN1 immunogold particles were generally located over vesicular compartments (Fig. 4b). In contrast, GluN1 immunogold in axon terminals forming excitatory-type synapses was often aligned along presynaptic membrane specializations on dendritic spines (Fig. 4c, d).

### Glial labeling for GluN1

GluN1 immunogold labeling was seen in many perisynaptic (Fig. 4e–i) and perivascular glial profiles. GluN1 immunogold particles in glia were most commonly seen at sites contacting the plasma membrane. The shape of GluN1-labeled glial profiles and their content of intermediate filaments are consistent with identification as astrocytes. GluN1-containing glial processes apposed dendritic profiles, many of which also contained GluN1 immuno-gold and/or D1 immunoperoxidase (Fig. 4e, f, i). Labeled glia frequently surrounded dendritic spines receiving asymmetric excitatory-type input. In some instances, the perisynaptic glial processes were enlarged and appeared to engulf the presynaptic axon terminal (Fig. 4i).

### Decreased density of dendritic GluN1 in the Acb core of isolation–reared rats

GluN1 immunogold density was significantly decreased in D1-containing dendrites of the Acb core of adult IR rats (group 3.94 ± 0.42; IR 2.70 ± 0.46, Welch's-corrected $t = 2.71$, $p = 0.02$; Fig. 5a). This isolation-induced decrease in GluN1 immunogold density was unique to dendrites of the Acb core that were dual-labeled for GluN1 and the D1 receptor. There was no significant difference between IR and group-housed rats in GluN1 immunogold in dendrites without D1, or in either singly-labeled or dual-labeled GluN1-containing profiles of the Acb shell (Fig. 5b).

### PPI deficit in isolation–reared rats

In IR adult rats, %PPI was significantly reduced below controls at the mid-range 6 dB prepulse intensity ($t(15) = 2.22$, $p = 0.04$; Fig. 6). This is similar to previous reports and has been replicated by many laboratories (for review, see Fone and Porkess 2008). Average %PPI, calculated as the average %PPI per animal in 3, 6, and 12 dB prepulse + pulse trials, did not significantly differ between groups ($t(15) = 1.389$, $p = 0.19$).

### GluN1 levels correlate with PPI

To test the hypothesis that glutamate receptor expression in the Acb accounts for individual variability of the PPI response, linear regression analysis was used to determine the statistical correlation between expression of post-synaptic GluN1 immunogold density and average %PPI across both rearing conditions. Separate analyses were undertaken for the Acb shell and core, and for dendrites that did and did not contain the dopamine D1 receptor. In both shell and core, there was a strong-positive correlation between average %PPI and GluN1 immunogold density in D1-containing dendrites (Fig. 7a, b). This correlation was more robust in the Acb shell ($r^2 = 0.49$, $p = 0.002$) than the core ($r^2 = 0.37$, $p = 0.009$).

Interestingly, in the Acb shell, there was also a signifi-cant positive correlation between average %PPI and GluN1 immunogold density in dendrites that did not contain the D1 receptor ($r^2 = 0.42$, $p = 0.005$). However, in the Acb core, no significant correlation existed between %PPI and GluN1 immunogold density in dendrites that were not dual-labeled with D1 immunoperoxidase. This finding may indicate regional specificity between the Acb core and shell regarding relative dopaminergic and glutamatergic modulation of the PPI response.

## Discussion

Using electron microscopic immunolabeling and behavioral testing, we conducted an in-depth study of the effect of adolescent social isolation on Acb glutamate and dopa-mine receptors. Overall expression patterns of these receptors were similar in isolates and group-reared adult rats: we observed GluN1 in axons and glia, and both GluN1 and D1 in somatodendritic profiles. However, we found that isolation rearing of rats throughout adolescence results in decreased density of GluN1 in dopamine-receptive dendrites of the Acb core. Notably, we report for the first time that endogenous GluN1 levels in D1-containing neurons of the Acb medial core and shell correlate with %PPI. These findings indicate that the adolescent social environment critically impacts glutamate receptors of the Acb and that the prepulse response directly correlates with this Acb glutamate receptor expression. Our findings show that Acb NMDA receptors are a biological substrate vulnerable to adolescent isolation, and provide a neurobiological rationale for adolescence as a critical period for social intervention.

### GluN1 localizes to dendrites, spines, axon terminals, glia, and D1R–containing somatodendritic profiles of the Acb core and shell

Electron microscopic immunolabeling revealed a distribution of GluN1 and D1 receptor immunolabeling in the ventromedial Acb core and shell of isolation-reared rats and socially housed controls similar to the distribution of these receptors reported in naive adult male rats (Hara and Pickel 2005). GluN1 immunogold particles were observed primarily not only within somatodendritic profiles and dendritic spines but also in axon terminals and glia. D1 immunoperoxidase was observed in somatodendritic profiles and spines, many of which also contained GluN1 immunogold.

The co-expression of D1R and GluN1 in smaller dendrites and dendritic spines is consistent with evidence that glutamatergic axon terminals form excitatory-type synapses on spiny dendrites receiving convergent input from dopaminergic axonal profiles (Sesack and Pickel 1992). These glutamatergic inputs derive extensively from the prefrontal cortex (PFC) and limbic brain regions including the lateral amygdala, which are respectively involved in cognitive and emotional processing and are differentially affected by IR (Rouillon et al. 2008; Schubert et al. 2009). The observed widespread co-localization of glutamate and D1 receptors in dendritic compartments of the Acb thereby directly facilitates the integration of the cortical and limbic signaling pathways affected by IR within the same neuron.

Acb axon terminals sometimes contained GluN1-immunogold, but not D1R immunoperoxidase. In both the core and shell, many of these singly labeled terminals formed asymmetric excitatory-type synapses on dendrites and dendritic spines, consistent with previous findings in the medial Acb shell (Gracy et al. 1997). NMDA receptors in these glutamate-containing axonal terminals may play a role in auto-inhibition; alternatively, given their frequent positioning near other excitatory-type terminals, these presynaptic NMDA receptors may facilitate cross-talk between axons. This suggests that coincident activation of presynaptic NMDA autoreceptors and postsynaptic NMDA receptors is involved in plasticity of glutamatergic synapses in the Acb, as has been shown for cortical inputs to the lateral amygdala (Froemke et al. 2003; Duguid and Sjostrom 2006).

GluN1 was also localized to perisynaptic glia, frequently on plasma membranes. This supports evidence of NMDA receptor involvement in the mediation of gliotrans-mission, which can drive bursts of action potentials in medium spiny neurons in the Acb (D'Ascenzo et al. 2007). We have specifically shown GluN1 labeling in perisynaptic glia contacting asymmetric excitatory-type synapses of dendritic spines that contain D1R and/or GluN1. Glial cells undergo substantial postnatal maturation, evidenced by increased vesicular glutamate transporter-1-labeled neuronal glutamatergic synapses ensheathed by astroglial processes (Morel et al. 2014). Because of this extensive glial postnatal maturation and the changes in neuronal NMDA receptor distribution we report in adolescent isolated rats, it is plausible that compensatory changes in glial GluN1 distribution and/or activity occur in IR adults; however, this is beyond the reach of the current study, as the irregular size and shape of glia precludes accurate analysis of immunogold density in glial profiles.

## Dendritic GluN1 density in D1–containing dendrites is decreased in isolates and is correlated with %PPI

We observed a significant IR-induced decrease in postsynaptic GluN1 in the motor-associated Acb core, but not the limbic-associated shell. We also report a strong-positive correlation between Acb dendritic GluN1 density and %PPI across all animals. Interestingly, in the Acb core, this correlation was significant only in D1-containing dendrites, while in the Acb shell, a significant positive correlation was observed in populations of dendrites both with and without the D1 receptor.

These observations point to subregion-specific differences in the relationship between glutamate and dopamine signaling in the Acb core and shell and PPI, which could differentially be affected by social isolation. This may be due to region-specific differences in afferents to the Acb core and shell or may reflect differing influences of Acb core and shell efferents on PPI circuitry.

The Acb integrates inputs from brain regions critical to limbic and cognitive regulation, including the hippocampus, paraventricular thalamus, amygdala, and prefrontal cortex (Kirouac 2015; Wright and Groenewegen 1995). While the Acb core and shell are both comprised principally of GABAergic medium spiny neurons, they are differentially targeted by dopaminergic and cortical glutamatergic projections. Dopaminergic projections of the ventral tegmental area (VTA) (Nirenberg et al. 1996; Salgado and Kaplitt 2015) innervate the shell, while the primary source of dopaminergic axon terminals in the core is the substantia nigra (Gerfen et al. 1987). The ventromedial prelimbic prefrontal, infralimbic, and posterior pyriform cortices extensively innervate the shell (Brog et al. 1993), while the core is preferentially targeted by glutamatergic projection neurons of the anterior cingulate, dorsal prelimbic, and perirhinal cortices (Groenewegen et al. 1999; Sesack et al. 1989). These prefrontal cortical inputs to the ventromedial Acb core and shell furthermore differentially target clusters of cells with high and low enkephalin content (Berendse et al. 1992). Cortical input to the Acb may additionally be gated by hippocampal afferents (O'Donnell and Grace 1995). The structural and functional development of these prefrontal regions continues into young adulthood (Casey and Jones 2010), and so their efferents may be uniquely vulnerable during adolescence to effects of the social environment. The selective

decrease in postsynaptic GluN1 in D1-containing dendrites of the Acb core could, therefore, reflect differential effects of IR on prefrontal regions targeting the core versus shell.

Our finding of decreased postsynaptic GluN1 density in the Acb of IR adult rats is consistent with a prior study showing that adolescent social isolation reduces somatic NMDA receptor expression in the Acb core and shell relative to rats raised under environmentally enriched conditions (Wood et al. 2005). Increased trans-Acb glutamate receptor expression resulting from the vastly differential experiences of adolescent environmental enrichment and social isolation may largely account for the regional discrepancy between our results and those of Wood et al. (2005). Our findings provide new evidence for a core-specific decrease in dendritic GluN1 when IR rats are compared to group-reared controls in otherwise the same environmental conditions.

The finding that %PPI correlates with endogenous GluN1 expression in the Acb shell and core is consistent with, and builds upon, pharmacological evidence implicating Acb glutamate and dopamine receptors in PPI regulation. Administration of NMDA receptor antagonists and dopamine receptor agonists directly into the Acb can produce similar PPI defects (Fone and Porkess 2008; Chavez et al. 2009). However, unlike pharmacologically induced PPI disruptions, which produce a pronounced deficit in each animal, isolation rearing induces a continuum of PPI responses appearing in a pattern similar to those observed in human psychiatric disorders (Braff et al. 2001). Our findings indicate that expression of Acb GluN1 explains much of the inter-subject variability in PPI deficits observed across both typical and affected populations, and that this is influenced by IR. Other factors in the social environment that could possibly contribute to the variability of PPI in our cohort include the social dominance hierarchy in cages of group-reared rats, birth order, and litter composition.

PPI, which measures sensorimotor gating, is a behavioral phenotype that fits criteria laid out by the Research Domain Criteria (RDoC), a framework introduced by the National Institute of Mental Health to refocus psychiatric disease research towards the inclusion of biological phenotypes (Insel 2014). PPI is a dimensional, transdiagnostic phenotype that can be measured across species and is appropriate for study of psychiatric disease ranging from genes and molecules through behavior and symptomology (Pineles et al. 2016). Although the circuitry contributing to the PPI response is complex and involves numerous brain regions, including the hippocampus and PFC (Swerdlow et al. 2001), our work identifies the GluN1 subunit of NMDA receptors in dopamine-responsive neurons of the Acb core and shell as one likely key molecular substrate of the PPI response, and provides rationale for NMDA receptors within the Acb as a specific molecular and anatomical target for therapeutic and imaging studies. This glutamate receptor population in both the Acb shell and core may furthermore be accessed by targeting the D1R, as we found that GluN1 in D1R-containing dendrites correlates with %PPI. Furthermore, the D1 receptor and GluN1 subunit directly interact through physical protein–protein associations (Fiorentini et al. 2003) and D1 activation induces trafficking of the NMDA receptor (Dunah and Standaert 2001). Because quinpirole, a dopa-mine D2 receptor agonist, impairs PPI when injected into the Acb (Wan and Swerdlow 1993), and prefrontal cortical D2 receptors are impacted by

isolation rearing (Fitzgerald et al. 2013), it would be interesting in future studies to examine pre- and postsynaptic accumbens D2 receptors in the context of isolation rearing.

This work exposes a developmental vulnerability of Acb glutamate receptors, a likely neural substrate of the PPI response, to the adolescent social environment. On the other hand, this same finding also identifies adolescence as an opportunity to change the developing brain, a critical period during which positive social interventions can have enduring effects on long-term adult psychiatric health in at-risk populations.

## Acknowledgements

The authors gratefully acknowledge the receipt of National Institute of Drug Abuse funding on Grants T32DA7274 to MLF and DA004600 to VMP, and National Institute of Mental Health funding on Grants T32MH15144 to MLF and MH40342 to VMP.

## References

Bakshi V, Geyer M (1999) Ontogeny of isolation rearing-induced deficits in sensorimotor gating in rats. Physiol Behav 67(3):385–392 [PubMed: 10497957]

Berendse H, Galis-de Graaf Y, Groenewegen H (1992) Topographical organization and relationship with ventral striatal compartments of prefrontal corticostriatal projections in the rat. J Comp Neurol 316(3):314–347 [PubMed: 1577988]

Braff D, Geyer M, Swerdlow N (2001) Human studies of prepulse inhibition of startle: normal subjects, patient groups, and pharmacological studies. Psychopharmacology 156(2–3):234–258 [PubMed: 11549226]

Broersen LM, Feldon J, Weiner I (1999) Dissociative effects of apo-morphine infusions into the medial prefrontal cortex of rats on latent inhibition, prepulse inhibition and amphetamine-induced locomotion. Neuroscience 94(1):39–46 [PubMed: 10613495]

Brog J, Salyapongse A, Deutch A, Zahm D (1993) The patterns of afferent innervation of the core and shell in the “accumbens” part of the rat ventral striatum: Immunohistochemical detection of retrogradely transported fluoro-gold. J Comp Neurol 338:255–278 [PubMed: 8308171]

Casey BJ, Jones RM (2010) Neurobiology of the adolescent brain and behavior. J Am Acad Child Adolesc Psychiatry 49(12):1189–1285. 10.1016/j.jaac.2010.08.017 [PubMed: 21093769]

Chavez C, Gogos A, Jones ME, van den Buuse M (2009) Psychotropic drug-induced locomotor hyperactivity and prepulse inhibition regulation in male and female aromatase knockout (ArKO) mice: role of dopamine D1 and D2 receptors and dopamine transporters. Psychopharmacology 206(2):267–279. 10.1007/s00213-009-1604-6 [PubMed: 19597801]

D’Ascenzo M, Fellin T, Terunuma M, Revilla-Sanchez R, Meaney DF, Auberson YP, Moss SJ, Haydon PG (2007) mGluR5 stimulates gliotransmission in the nucleus accumbens. Proc Natl Acad Sci USA 104(6):1995–2000. 10.1073/pnas.0609408104 [PubMed: 17259307]

Day-Wilson KM, Jones DNC, Southam E, Cilia J, Totterdell S (2006) Medial prefrontal cortex volume loss in rats with isolation rearing-induced deficits in prepulse inhibition of acoustic startle. Neuroscience 141(3):1113–1121. 10.1016/j.neuroscience.2006.04.048

Duguid I, Sjostrom PJ (2006) Novel presynaptic mechanisms for coincidence detection in synaptic plasticity. Curr Opin Neurobiol 16(3):312–322.10.1016/j.conb.2006.05.008 [PubMed: 16713246]

Dunah AW, Standaert DG (2001) Dopamine D1 receptor-dependent trafficking of striatal NMDA glutamate receptors to the postsynaptic membrane. J Neurosci 21(15):5546–5558 [PubMed: 11466426]

Fiorentini C, Gardoni F, Spano P, Di Luca M, Missale C (2003) Regulation of dopamine D1 receptor trafficking and desensitization by oligomerization with glutamate N-methyl-d-aspartate receptors. J Biol Chem 278(22):20196–20202 [PubMed: 12646556]

Fitzgerald ML, Mackie K, Pickel VM (2013) The impact of adolescent social isolation on dopamine D2 and cannabinoid CB1 receptors in the adult rat prefrontal cortex. Neuroscience 235:40–50. 10.1016/j.neuroscience.2013.01.021 [PubMed: 23333674]

Fone KC, Porkess MV (2008) Behavioural and neurochemical effects of post-weaning social isolation in rodents-relevance to developmental neuropsychiatric disorders. Neurosci Biobehav Rev 32(6): 1087–1102.10.1016/j.neubiorev.2008.03.003 [PubMed: 18423591]

Froemke R, Li C, Dan Y (2003) A form of presynaptic coincidence detection. Neuron 39(4):579–581 [PubMed: 12925271]

Gerfen CR, Herkenham M, Thibault J (1987) The neostriatal mosaic: II. Patch- and matrix-directed mesostriatal dopaminergic and nondopaminergic systems. J Neurosci 7(12):3915–3934 [PubMed: 2891799]

Glass MJ, Lane DA, Colago EE, Chan J, Schlussman SD, Zhou Y, Kreek MJ, Pickel VM (2008) Chronic administration of morphine is associated with a decrease in surface AMPA GluR1 receptor subunit in dopamine D1 receptor expressing neurons in the shell and non-D1 receptor expressing neurons in the core of the rat nucleus accumbens. Exp Neurol 210(2):750–761. 10.1016/j.expneurol.2008.01.012 [PubMed: 18294632]

Gracy KN, Pickel VM (1996) Ultrastructural immunocytochemical localization of the N-methyl-d-aspartate receptor and tyrosine hydroxylase in the shell of the rat nucleus accumbens. Brain Res 739(1–2):169–181 [PubMed: 8955937]

Gracy K, Svingos A, Pickel V (1997) Dual ultrastructural localization of mu-opioid receptors and NMDA- type glutamate receptors in the shell of the rat nucleus accumbens. J Neurosci 17(12): 4839–4848 [PubMed: 9169542]

Groenewegen HJ, Wright CI, Beijer AV, Voorn P (1999) Convergence and segregation of ventral striatal inputs and outputs. Ann N Y Acad Sci 877:49–63 [PubMed: 10415642]

Hara Y, Pickel V (2005) Overlapping intracellular and differential synaptic distributions of dopamine D1 and glutamate N-methyl-d-aspartate receptors in rat nucleus accumbens. J Comp Neurol 492(4):442–455 [PubMed: 16228995]

Hara Y, Pickel (2009) Preferential relocation of the N-methyl-d-aspartate receptor NR1 subunit in nucleus accumbens neurons that contain dopamine D1 receptors in rats showing an apo-morphine-induced sensorimotor gating deficit. Neuroscience 154(3):965–977

Insel TR (2014) The NIMH Research Domain Criteria (RDoC) Project: precision medicine for psychiatry. Am J Psychiatry 171(4):395–397. 10.1176/appi.ajp.2014.14020138 [PubMed: 24687194]

Kirouac GJ (2015) Placing the paraventricular nucleus of the thalamus within the brain circuits that control behavior. Neurosci Biobehav Rev 56:315–329. 10.1016/j.neubiorev.2015.08.005 [PubMed: 26255593]

Leranth C, Frotscher M (1989) Organization of the septal region in the rat brain: cholinergic-GABAergic interconnections and the termination of hippocampo-septal fibers. J Comp Neurol 289(2):304–314. 10.1002/cne.902890210 [PubMed: 2808769]

Levey A, Hersch S, Rye D, Sunahara R, Niznik H, Kitt C, Price D, Maggio R, Brann M, Ciliax B (1993) Localization of D1 and D2 dopamine receptors in brain with subtype-specific antibodies. Proc Natl Acad Sci USA 90(19):8861–8865 [PubMed: 8415621]

Milner TA, Waters EM, Robinson DC, Pierce JP (2011) Degenerating processes identified by electron microscopic immunocytochemical methods In: Giovanni Manfredi HK (ed) Neurodegeneration: methods and protocols, vol 793. Methods in molecular biology, 1st edn. Humana Press, New York, pp 23–59. 10.1007/978-1-61779-328-8_3

Morel L, Higashimori H, Tolman M, Yang Y (2014) VGluT1 + neuronal glutamatergic signaling regulates postnatal developmental maturation of cortical protoplasmic astroglia. J Neurosci 34(33): 10950–10962. 10.1523/JNEUROSCI.1167-14.2014 [PubMed: 25122895]

Nirenberg MJ, Chan J, Liu Y, Edwards RH, Pickel VM (1996) Ultrastructural localization of the vesicular monoamine transporter-2 in midbrain dopaminergic neurons: potential sites for somatodendritic storage and release of dopa-mine. J Neurosci 16 (13):4135–4145. 10.1002/(SICI)1096-9861(19960715)371:1<116::AID-CNE7>3.0.CO;2-6 [PubMed: 8753875]

O'Donnell P, Grace AA (1995) Synaptic interactions among excitatory afferents to nucleus accumbens neurons: hippocampal gating of prefrontal cortical input. J Neurosci 15(5 Pt 1):3622–3639 [PubMed: 7751934]

Paxinos G, Watson C (1998) The rat brain in stereotaxic coordinates. Academic Press, San Diego

Pineles SL, Blumenthal TD, Curreri AJ, Nillni YI, Putnam KM, Resick PA, Rasmusson AM, Orr SP (2016) Prepulse inhibition deficits in women with PTSD. Psychophysiology 53(9):1377–1385. 10.1111/psyp.12679 [PubMed: 27237725]

Powell SB, Geyer MA, Preece MA, Pitcher LK, Reynolds GP, Swerdlow NR (2003) Dopamine depletion of the nucleus accumbens reverses isolation-induced deficits in prepulse inhibition in rats. Neuroscience 119(1):233–240 [PubMed: 12763084]

Ramocki MB, Zoghbi HY (2008) Failure of neuronal homeostasis results in common neuropsychiatric phenotypes. Nature 455(7215):912–918. 10.1038/nature07457 [PubMed: 18923513]

Reijmers LG, Vanderheyden PM, Peeters BW (1995) Changes in pre-pulse inhibition after local administration of NMDA receptor ligands in the core region of the rat nucleus accumbens. Eur J Pharmacol 272(2–3):131–138 [PubMed: 7713156]

Rouillon C, Abraini J, David H (2008) Prefrontal cortex and basolateral amygdala modulation of dopamine-mediated locomotion in the nucleus accumbens core. Exp Neurol 212(1):213–217 [PubMed: 18501353]

Salgado S, Kaplitt MG (2015) The nucleus accumbens: a comprehensive review. Stereotact Funct Neurosurg 93(2):75–93. 10.1159/000368279 [PubMed: 25720819]

Schubert MI, Porkess MV, Dashdorj N, Fone KC, Auer DP (2009) Effects of social isolation rearing on the limbic brain: a combined behavioral and magnetic resonance imaging volumetry study in rats. Neuroscience 159(1):21–30. 10.1016/j.neuroscience.2008.12.019 [PubMed: 19141315]

Sebastian C, Viding E, Williams KD, Blakemore SJ (2010) Social brain development and the affective consequences of ostracism in adolescence. Brain Cogn 72(1):134–145. 10.1016/j.bandc.2009.06.008 pii] [PubMed: 19628323]

Sesack SR, Pickel VM (1992) Prefrontal cortical efferents in the rat synapse on unlabeled neuronal targets of catecholamine terminals in the nucleus accumbens septi and on dopamine neurons in the ventral tegmental area. J Comp Neurol 320(2):145–160. 10.1002/cne.903200202 [PubMed: 1377716]

Sesack S, Deutch A, Roth R, Bunney B (1989) Topographic organization of the efferent projections of the medial prefrontal cortex in the rat: an anterograde tract-tracing study with Phaseolus vulgaris leucoagglutinin. J Comp Neurol 290:213–242 [PubMed: 2592611]

Somerville LH, Jones RM, Casey BJ (2010) A time of change: behavioral and neural correlates of adolescent sensitivity to appetitive and aversive environmental cues. Brain Cogn 72(1):124–133. 10.1016/j.bandc.2009.07.003 [PubMed: 19695759]

Spear LP (2000) The adolescent brain and age-related behavioral manifestations. Neurosci Biobehav Rev 24(4):417–463 [PubMed: 10817843]

Swerdlow N, Braff D, Masten V, Geyer M (1990) Schizophrenic-like sensorimotor gating abnormalities in rats following dopamine infusion into the nucleus accumbens. Psychopharmacology 101(3):414–420 [PubMed: 2114026]

Swerdlow N, Braff D, Geyer M (2000) Animal models of deficient sensorimotor gating: what we know, what we think we know, and what we hope to know soon. Behav Pharmacol 11(3–4):185–204 [PubMed: 11103873]

Swerdlow NR, Geyer MA, Braff DL (2001) Neural circuit regulation of prepulse inhibition of startle in the rat: current knowledge and future challenges. Psychopharmacology 156(2–3):194–215 [PubMed: 11549223]

Swerdlow N, Light G, Cadenhead K, Sprock J, Hsieh M, Braff D (2006) Startle gating deficits in a large cohort of patients with schizophrenia: relationship to medications, symptoms, neurocognition, and level of function. Arch Gen Psychiatry 63(12):1325–1335 [PubMed: 17146007]

Wan FJ, Swerdlow NR (1993) Intra-accumbens infusion of quinpirole impairs sensorimotor gating of acoustic startle in rats. Psychopharmacology 113(1):103–109 [PubMed: 7862814]

Wilkinson LS, Killcross SS, Humby T, Hall FS, Geyer MA, Robbins TW (1994) Social isolation in the rat produces developmentally specific deficits in prepulse inhibition of the acoustic startle response without disrupting latent inhibition. Neuropsychopharmacology 10(1):61–72. 10.1038/npp.1994.8 [PubMed: 8179795]

Wood D, Buse J, Wellman C, Rebec G (2005) Differential environmental exposure alters NMDA but not AMPA receptor subunit expression in nucleus accumbens core and shell. Brain Res 1042(2): 176–183 [PubMed: 15854589]

Wright CI, Groenewegen HJ (1995) Patterns of convergence and segregation in the medial nucleus accumbens of the rat: relationships of prefrontal cortical, midline thalamic, and basal amygdaloid afferents. J Comp Neurol 361(3):383–403 [PubMed: 8550887]

Zahm D (2000) An integrative neuroanatomical perspective on some subcortical substrates of adaptive responding with emphasis on the nucleus accumbens. Neurosci Biobehav Rev 24(1):85–105 [PubMed: 10654664]

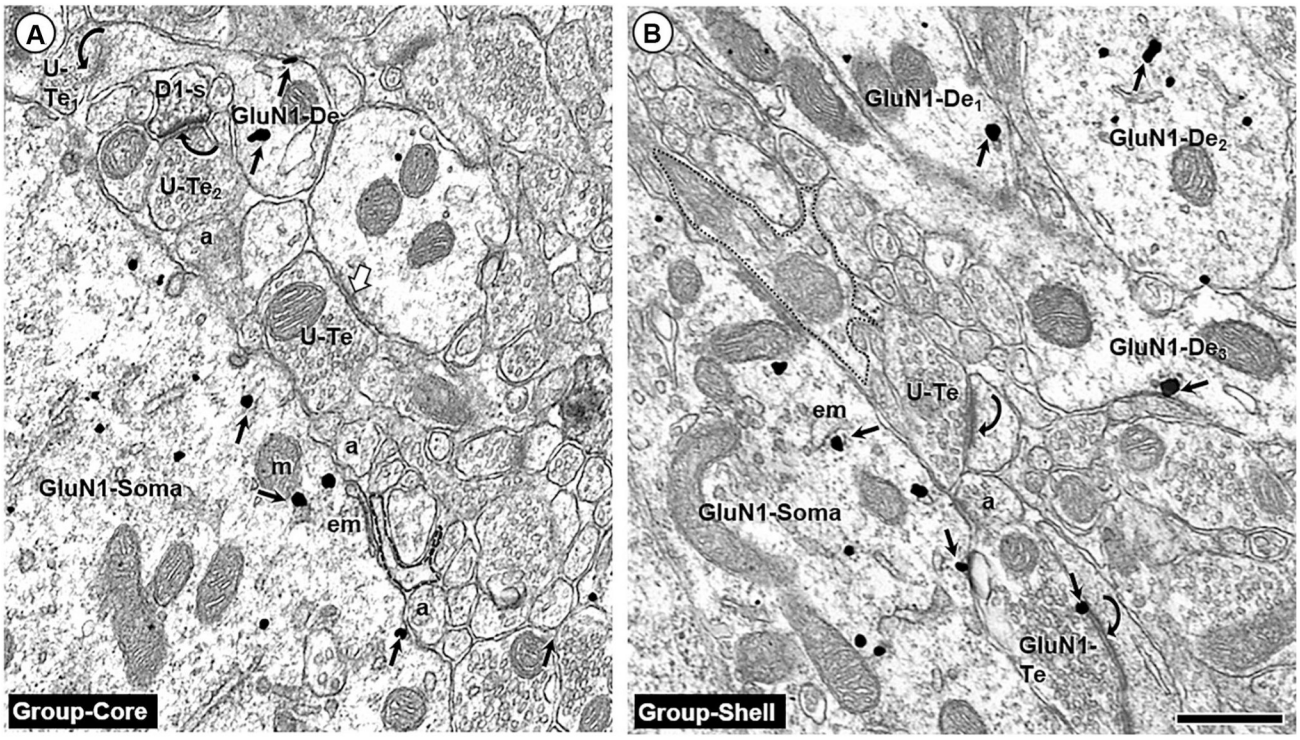


**Fig. 1.**

Somatodendritic GluN1 labeling. Endomembranes (em) and non-synaptic plasma membranes contain GluN1 immunogold (small arrows) in soma (GluN1-Soma) and dendrites (GluN1-De) of the Acb core (**a**) and shell (**b**) of group-reared adult rats. These profiles are without detectable D1R-immunoperoxidase labeling such as that seen in a nearby dendritic spine (D1-s) in **a**. Nearby terminals are unlabeled (U-Te) or GluN1-labeled (GluN1-Te) and form asymmetric (curved arrows) or symmetric (white block arrow) with nearby dendritic profiles that are largely unlabeled. The labeled soma and dendrites are apposed by many small axonal (**a**) and glial profiles (outlined with a dashed line); scale bar = 500 nm

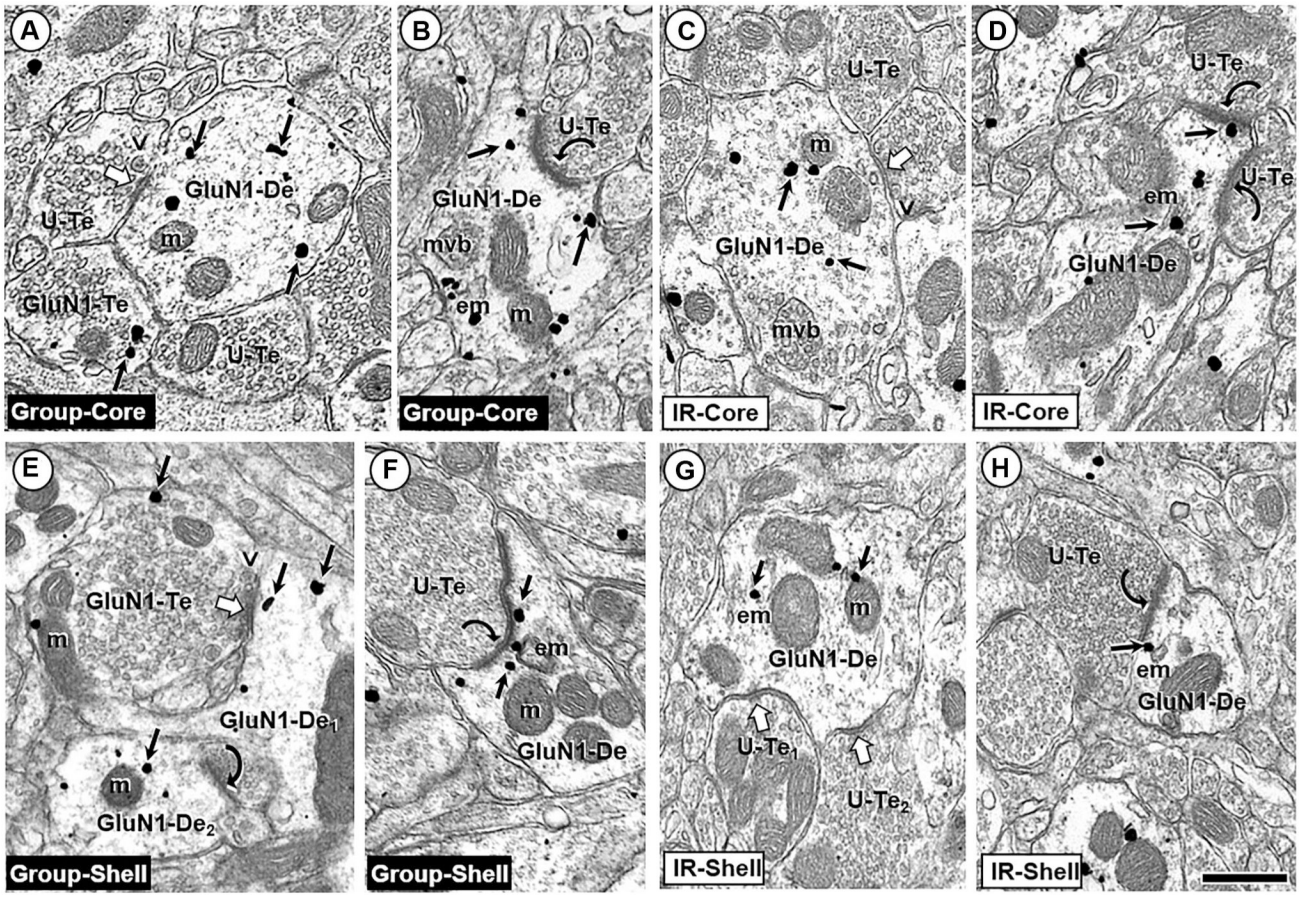


**Fig. 2.**

Singly labeled GluN1 dendritic profiles. Small arrows show GluN1 immunogold distribution in dendritic shafts (GluN1-De) without D1R immunoreactivity in the Acb core (**a–d**) and shell (**e–h**). In each rearing condition, the immunogold particles in both Acb compartments are seen mainly near cytoplasmic endomembranes (em) and mitochondria (m) in dendritic profiles receiving symmetric synapses (white block arrows), and within or near postsynaptic membrane specializations at asymmetric synapses (curved arrows) formed by unlabeled axon terminals (U-Te). The terminals forming symmetric synapses frequently contain many small clear vesicles and a few isolated large dense-core vesicles (v). Some of these terminals were also labeled for GluN1 immunogold (GluN1-Te). Note qualitatively similar levels of dendritic GluN1 immunogold particles in electron micrographs from IR and group-housed rats. *mvb* multivesicular body; scale bar = 500 nm

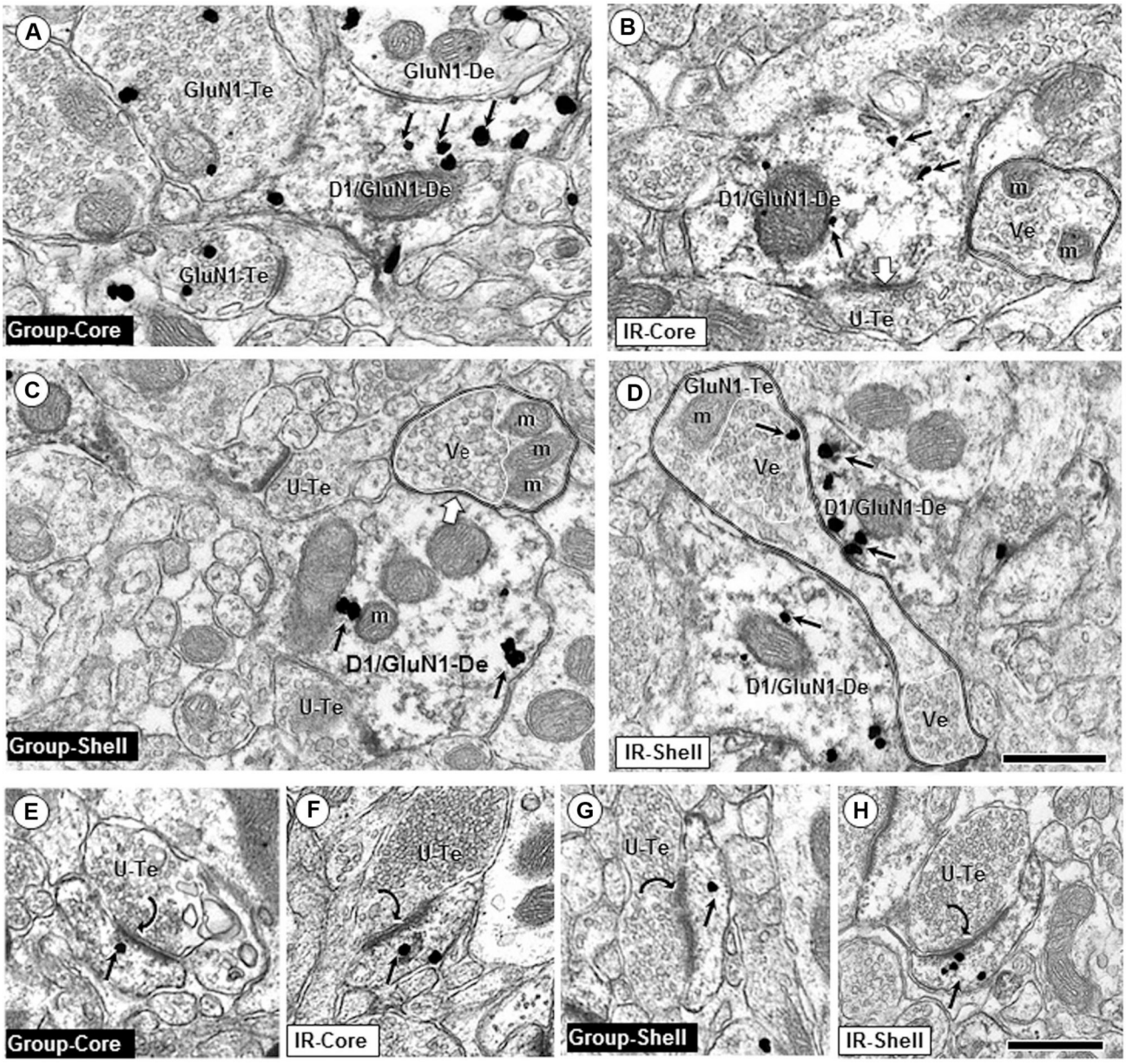


**Fig. 3.**

Dendritic shaft and spine profiles dual labeled for GluN1 and D1. In dendritic shafts, GluN1 immunogold is frequently located near endomembranes (em) and mitochondria (m) and less commonly on non-synaptic portions of the plasma membranes in profiles from group-reared (**a, c**) and IR (**b, d**). Axon terminals apposing these dendrites are often unlabeled (U-Te; **b, c**) but sometimes also contain GluN1 immunogold (GluN1-Te; **a, d**). Unlabeled axon terminals identified by double black lines show partially segregated compartmental distributions of densely packed vesicles (Ve, white line) and mitochondria (m). In **D**, two dually labeled dendrites are contacted by an “en passant” axon terminal (GluN1-Te) with two clusters of vesicles (see Gracy and Pickel 1996 for comparison with dopamine axons in the Acb shell). Note the qualitative decrease of GluN1 immuno-gold (small arrows) in IR

rats in dendritic shafts co-expressing D1Rs (D1/GluN1-De) in the Acb core (**a, b**), but not in dually labeled dendritic shafts in the shell (**c, d**). **e–h** show dually labeled spines in core or shell of IR and control adult rats; scale bar = 500 nm

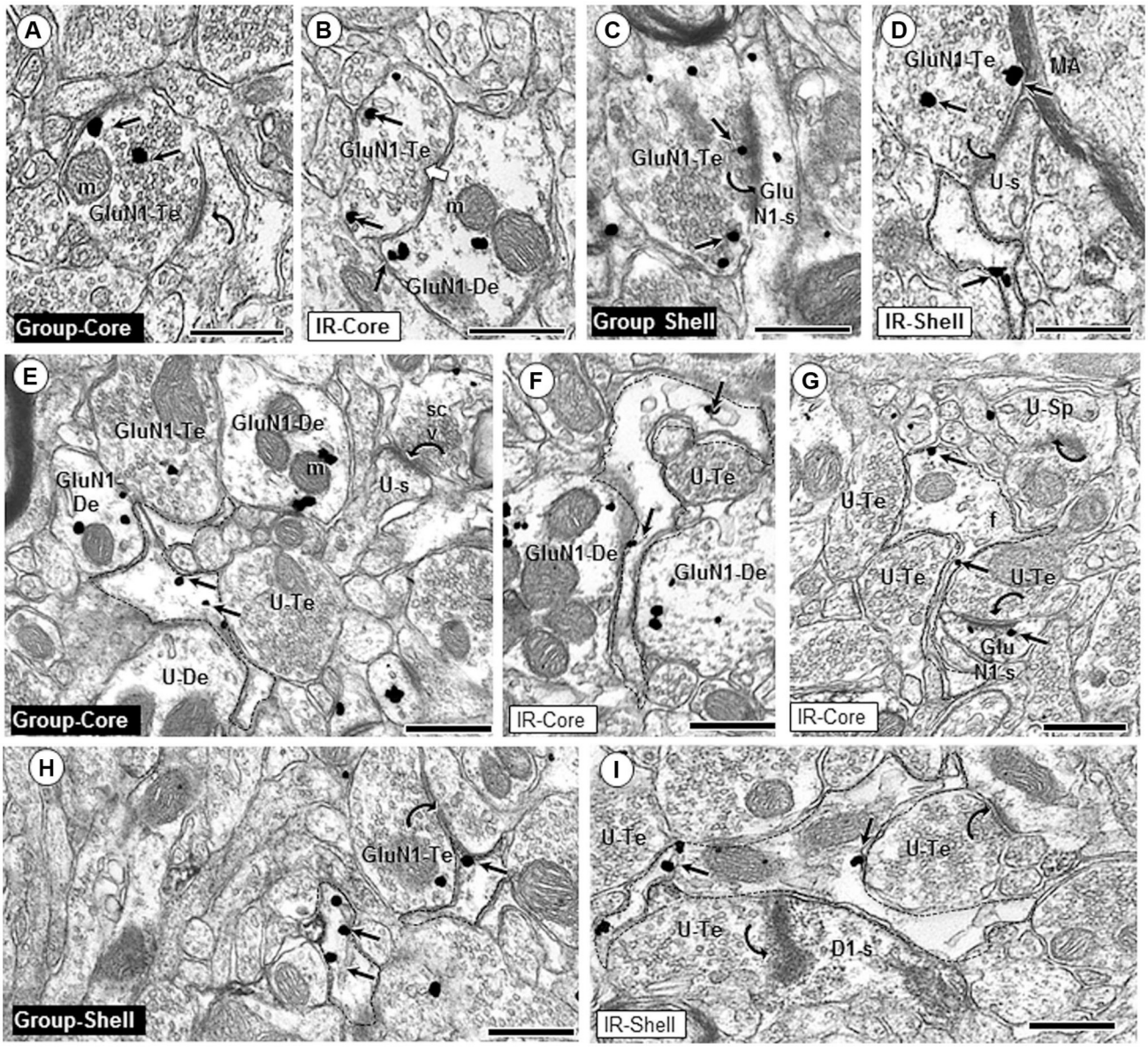


**Fig. 4.**

Glial and axonal GluN1 expression. GluN1 immunogold particles are present in axonal (**a–d**) and glial (**e–i**) profiles in the Acb core and shell of group- and isolation (IR)-reared adult rats. GluN1 immunogold particles (small arrows) are frequently in contact with non-synaptic plasma membranes in the interior of axon terminals (GluN1-Te; **a, d, h**), or localize near the synaptic active zone (**c**). GluN1-containing axon terminals often form asymmetric synapses (curved arrows; **a, c, d**) with dendritic spines in the Acb core and shell of both group and IR animals. GluN1 immunogold is also seen in axon terminals forming symmetric synapses (white block arrow, **b**). In both regions, GluN1 immunogold labeling is seen in filamentous glial processes (dashed outline; **e–i**) apposing unlabeled (U-Te; **e, f, g**) and GluN1-labeled (**h, i**) axon terminals, as well as unlabeled dendrites (U-De; **e**) and GluN1-labeled dendrites (GluN1-De; **f**). Asymmetric axospinous synapses (curved arrows) are typically seen in the

neuropil near GluN1-labeled glial profiles (**g, h, i**). *m* mitochondria, *U-s* unlabeled spine, *scv* small clear vesicles, *f* intermediate filament; scale bar = 500 nm

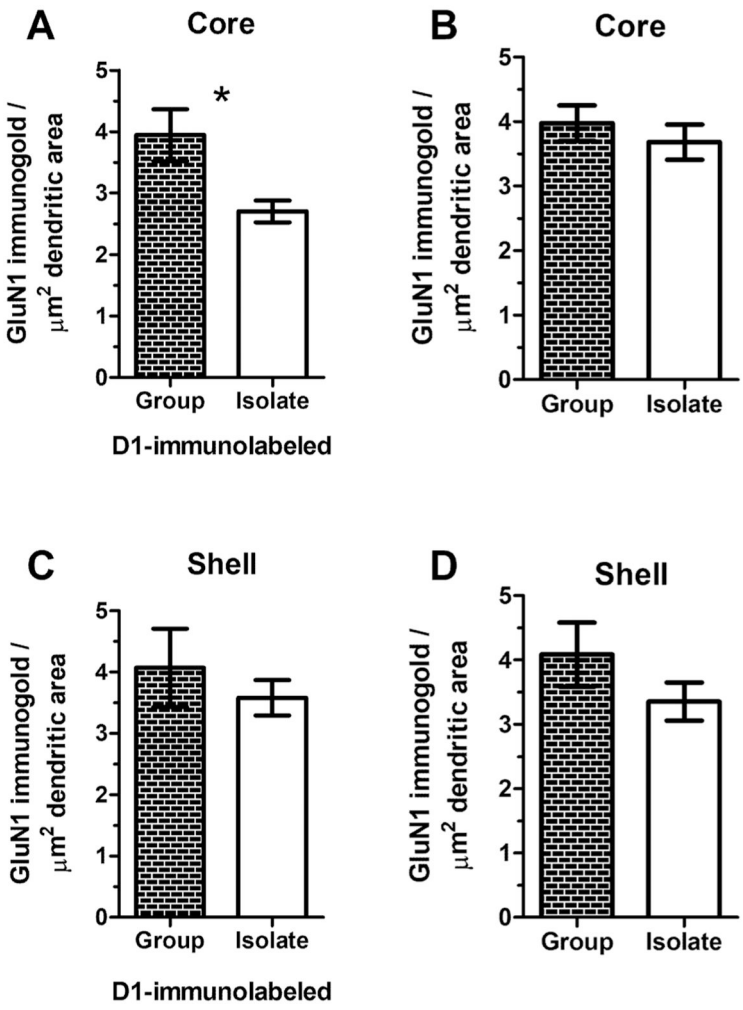


**Fig. 5.**

Region-specific reduction of GluN1 immunogold in D1R-labeled dendritic profiles in the Acb core of IR male rats. In the Acb core (**a**), isolation rearing induces a significant decrease in GluN1 immunogold density in dendrites that are also immunolabeled for the dopamine D1 receptor ($t(16) = 2.71$, $p = 0.02$) but not in dendrites that do not contain the D1 receptor (**b**). However, in the Acb shell, there is no significant between-group difference in dendritic density of GluN1 immunogold particles either in dendrites that contain the D1 receptor (**c**) or those that do not (**d**)

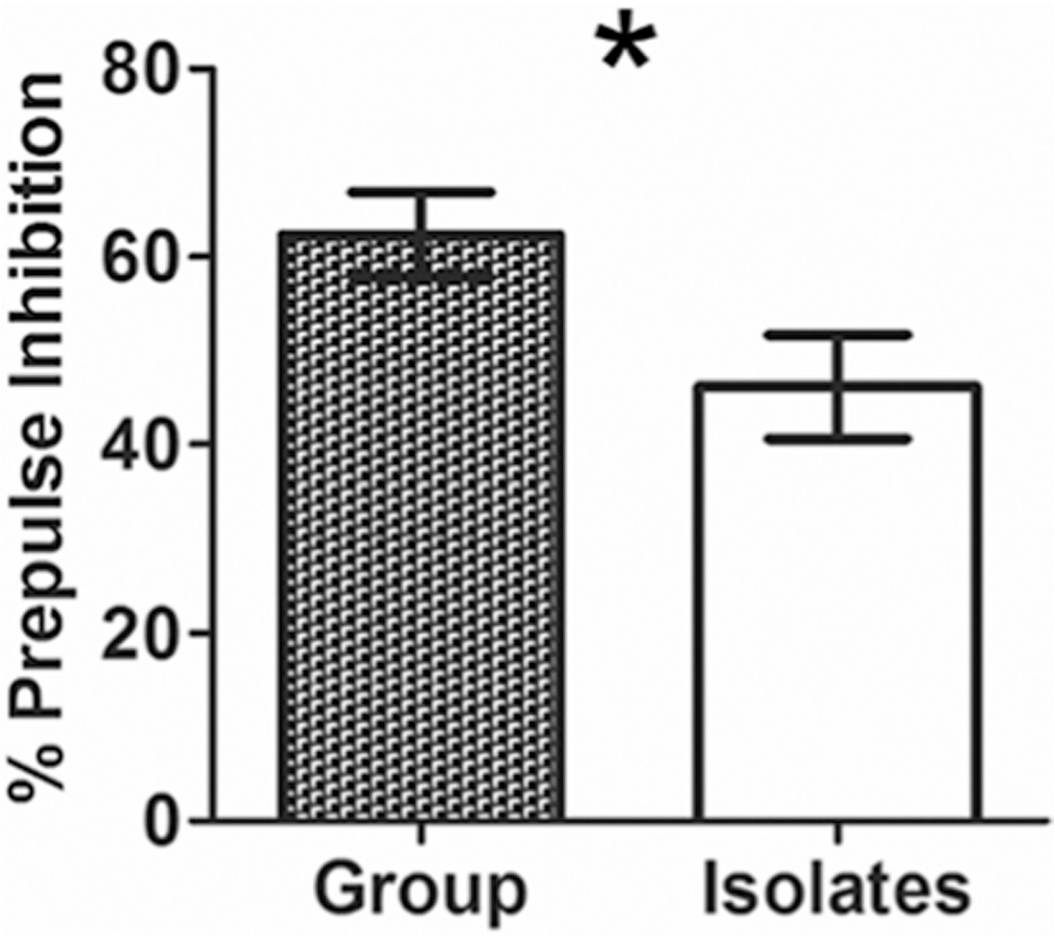


**Fig. 6.**

Decreased prepulse inhibition (PPI) of acoustic startle in isolation-reared adult male rats. A significant (asterisk) deficit in isolated rats is observed at the 6 decibel (dB) prepulse intensity ($t(15) = 2.22$, $p = 0.04$)

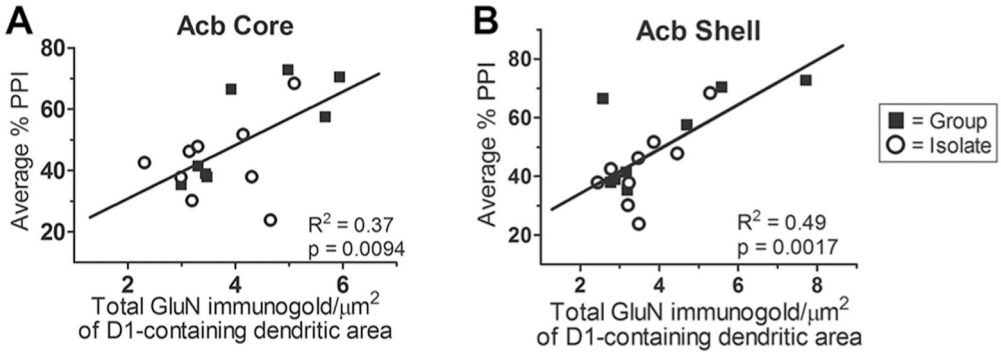


**Fig. 7.**

Correlation between average % PPI and GluN1 density in D1R-containing dendrites in the Acb. Average % PPI significantly correlates with total GluN1 immunogold in D1-containing dendrites ($r^2 = 0.37$, $p = 0.009$) within the Acb core (**a**) across both IR- and group-reared rats. Similarly, in the Acb shell (**b**), average %PPI significantly correlates with total GluN1 immunogold in D1-containing dendrites ($r^2 = 0.49$, $p = 0.002$)